Quantum Walk Experiments Using a 32 × 32 Silicon Photonic Path-Independent Insertion Loss Switch as a Stable Multiport Interferometer

Ryotaro Konoike, Akio Yoshizawa, Shu Namiki, *Fellow, IEEE*, and Kazuhiro Ikeda, *Member, IEEE*

(Integrated Photonics 2022)

***Abstract*—We study a 32 × 32 silicon photonic path-independent insertion loss switch used as a programmable multiport interferometer, with a robustness to optical losses appropriate for many classical and quantum photonic applications since any route through the interferometer has the same loss. Its operation stability was investigated by monitoring the fidelity (closeness to the ideal case) of single-photon quantum-walk experiments, where heralded single photons with a 10-nm bandwidth centered at 1547 nm were used as walkers in the interferometer. Fidelities of 0.98 and 0.97 were observed for 4- and 8-step quantum walks, respectively. The experiment took 21 hours to collect the data for the fidelity calculations. Similar fidelities were confirmed using narrowband classical light sources (200-kHz linewidth), for which a fidelity degradation as small as 10^{-5}/hour was achieved in the 45-hour free-running operation. The experiments demonstrate that our optical circuit has a wide range of potential applications to classical and quantum photonic processors based on a multiport input–output interference design.**

***Index Terms*—Integrated optics, quantum circuit, quantum optics, silicon photonics.**

I. Introduction

RECENTLY, photonic integrated circuits (PICs) have been of crucial importance in photon-based quantum information processing (QIP) applications as they offer the integration of many optical components on a chip, allowing large-scale realization of photon-based quantum experiments, which are difficult to conduct in free space [1], [2]. Reconfigurable PICs are especially useful as they can be adapted to many applications, making them multi-purpose or universal platforms for quantum photonic experiments [3]. Moreover, they also offer tolerances to fabrication and/or environmental errors, which often arise in complex systems, making them tolerant to complex and large-scale experiments.

Previously, a universal linear chip for quantum experiments was demonstrated using an array of reconfigurable Mach–Zehnder interferometers (MZIs) on a silica waveguide platform [3]. Compared to bulk interferometric systems [4], on-chip optical circuits with reconfigurable MZIs are very flexible as they allow small granular settings of each MZI. Recently, silicon (Si) photoics-based platforms have attracted interest because they offer much denser integration of optical components than silica waveguide platforms due to the large refractive index of Si [2], [5]. Therefore, the Si photonics platform is considered to be suitable for lage-scale applications. However, there are two points regarding the Si photonics platform that have not been addressed in previous experiments. One is waveguide dispersion, which limits the possible operation bandwidth, making the use of broadband photons generated through nonlinear optical effect difficult. The second point is the temporal stability of configured optical circuits on the platform, which is especially important for quantum experiments that require long integration times. In this paper, we address these issues using an actual Si photonics large-scale circuit and single photons.

In this paper, we focus on the quantum walk (QW), which is the quantum counterpart of the classical random walk. In a one-dimensional classical random walk, a particle changes its direction (left and right) randomly and the resulting probability of finding the particle in a specified position exhibits a Gaussian distribution. On the other hand, a quantum particle (or probability amplitude) in a QW splits into two possible directions of equal weight (in the case of a Hadamard walk), which interfere with each other, resulting in a non-Gaussian probability distribution. This fundamental difference makes possible many interesting applications of a QW, such as platforms for quantum transport simulations and tools for building efficient quantum computing algorithms [5], [6], [7], [8], [9], [10].

Specifically, photonic circuits can implement a QW by using optical splitters and phase shifters. A QW implemented with discrete splitters is called a *discrete-time* QW, and has the advantage of allowing tuning of each splitter element. By utilizing such discrete photonic QW circuits, researchers have realized quantum transport simulations of phenomena such as Anderson localization [1], [5], [9]. However, we consider that there are still issues regarding the further scaling of photonic circuits, because their bandwidth characteristics and long-time stability were not clarified in previous studies. These characteristics are clearly very important, as photons naturally have

Manuscript received 30 May 2022; revised 2 September 2022; accepted 7 September 2022. Date of publication 12 September 2022; date of current version 16 December 2022. *(Corresponding author: Ryotaro Konoike.)*

The authors are with the Platform Photonics Research Center, National Institute of Advanced Industrial Science and Technology (AIST), Tsukuba 305-8568, Japan (e-mail: r.konoike@aist.go.jp; yoshizawa-akio@aist.go.jp; shu.namiki@aist.go.jp; kaz.ikeda@aist.go.jp).

Color versions of one or more figures in this article are available at https://doi.org/10.1109/JLT.2022.3205624.

Digital Object Identifier 10.1109/JLT.2022.3205624

This work is licensed under a Creative Commons Attribution 4.0 License. For more information, see https://creativecommons.org/licenses/by/4.0/

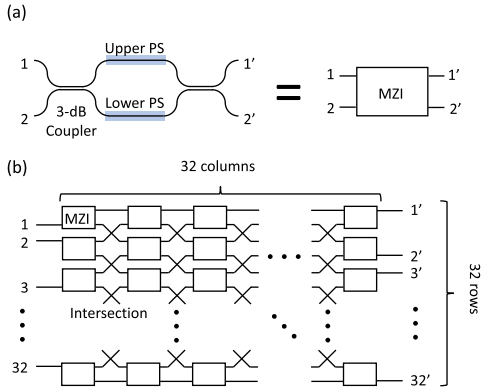

Fig. 1. Schematic structures of (a) MZI and (b) 32 × 32 path-independent insertion loss (PILOSS) optical switch. PS = Phase shifter, MZI = Mach-Zehnder interferometer.

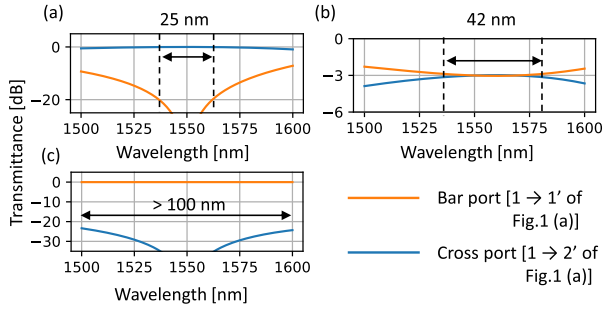

Fig. 2. Calculated transmission spectra for (a) cross, (b) 3-dB and (c) bar states of an MZI.

broad spectra originating from nonlinear optical processes, and long-term stability is necessary for many quantum experiments that require long integration times to obtain sufficient photon counts.

Recently, we have demonstrated a 32 × 32 Si photonics-based strictly non-blocking optical switch consisting of 1,024 MZIs on a chip based on path-independent insertion loss (PILOSS) topology, as shown in Figs. 1(a) and 1(b) [11], [12]. In the PILOSS topology, all possible optical paths have the same insertion loss (and length) from input to output. We also developed an electric circuit board equipped with field programmable gate arrays (FPGAs) to control 2,048 TO heaters on a chip, together with electrical/optical packaging techniques. This allowed us to characterize all 32 × 32 path transmissions, which was the first realization of full-path operation of a 32 × 32 optical switch [13].

The uniform insertion loss between paths exhibited by the PILOSS topology is preferable for use in quantum interference circuits such as those using QWs. Similar circuit designs with the same number of optical components in each path can also be used as a robust photonic unitary circuit, as shown in [14]. In this paper, we utilize a 32 × 32 optical switch circuit as a reconfigurable discrete-time QW circuit and experimentally demonstrate 1- to 8-step QWs with single photons generated through spontaneous parametric down conversion (SPDC). From these results, we experimentally verify both the bandwidth and long-time stability of large-scale quantum photonic circuits. Previously, we have preliminary reported the formation of QW circuits on the Si photonics circuit [15]. However, theory about the phase error trimming and the quantitative analyses has been lacked. In this paper, we show the detailed operation principle, the trimming methods of the device, and the details about the experimental results with qualitative analyses of them.

When using only one 'walker' and only measuring the statistical distribution of photons, the results can also be understood by 'classical' interferograms, i.e., classical light such as coherent light would reproduce the same results. In fact, some previous demonstrations of optical quantum walks have used classical light [5], [6]. In this paper, we use heralded single photons to show the bandwidth and stability of the platform with actual quantum particles, and we do not focus on the properties of single photons. Therefore, it is acceptable to use one 'walker' and measure the distribution of photons. We note that to determine the quantum properties of the photons, we could measure the correlation of photons between different ports, and we intend to address this in future work.

In Section II, we show the detailed structure of the device and the method to construct QW circuits with the switch. In Section III, we describe a method to trim phase errors originating from fabrication errors. The results of single-photon QWs and the temporal stability are shown in Section IV. In Section V, we discuss scaling of the device. Finally, Section VI concludes the paper.

II. Device Structure

Fig. 1(a) shows the schematic structure of an MZI. The MZI consists of two TO phase shifters between two 3-dB couplers based on directional couplers. The two (upper and lower) phase shifters can be controlled independently. The intersection is based on a single-layer crossing of two adiabatically expanded waveguides to reduce loss and crosstalk [16]. Fig. 1(b) shows the schematic structure of the 32 × 32 optical switch. The 32 × 32 matrix of MZIs is connected by intersections. Although the device has 64 optical modes, as shown in this figure, this PILOSS topology accepts only 32 ports for switching.

By adjusting the phase difference between the two phase shifter arms in Fig. 1(a), an MZI can be used as a variable beam splitter. Fig. 2 shows transmission spectra of three representative MZI states. Fig. 2(a) shows spectra of a state called the *cross* state, obtained when $1 \rightarrow 2'$ and $2 \rightarrow 1'$ in Fig. 1(a) are connected, and the phase difference between the two phase shifters is zero. The bandwidth for 20-dB suppression of the leakage is 25 nm centered at 1550 nm. We calculated these spectra using the finite element method (FEM) and coupled mode theory (CMT). Fig. 2(b) shows spectra of a state called the *3-dB* state, which can be used as a beam splitter, when the phase difference is $\pi/2$. The 0.1-dB deviation bandwidth is 42 nm. Finally, Fig. 2(c) shows spectra of the *bar* state, in which $1 \rightarrow 1'$, $2 \rightarrow 2'$ are connected. The bandwidth for the *bar* state have been measured in our previous publication [17]. From these results, we can expect that an MZI can be used as a variable beam splitter with a bandwidth of tens of nanometers.

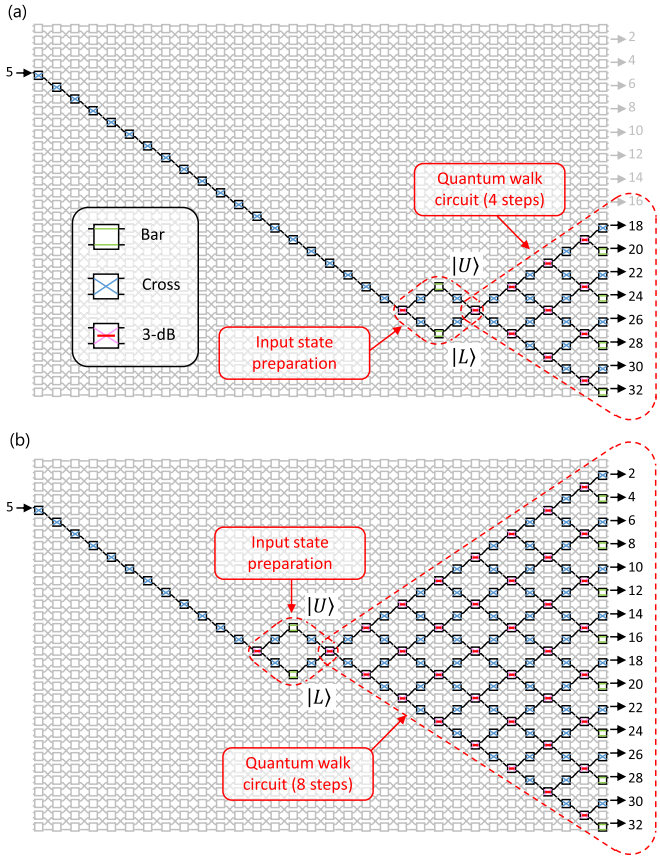

Fig. 3. Schematic illustration of (a) 4- and (b) 8-step QW circuit configurations for 32 × 32 PILOSS optical switch.

We configured each MZI in the 32 × 32 switch to construct 1- to 8-step QW circuit configurations, as shown in Figs. 3(a) and 3(b), for a 4- and 8-step QW, respectively. As shown in Fig. 3(b), the number of required output ports is 16 for an 8-step quantum walk. Therefore, we measured only these 16 output ports with leaving the other ports unused. We input single photons from input port 5, and the photons were guided to the input preparation part to create a superposition state $(1/\sqrt{2})(|U\rangle + |L\rangle)$. Here, $|U\rangle$ and $|L\rangle$ represent single-photon states for the upper and lower paths, respectively. Then, cascaded 3-dB beam splitters were used to construct a QW circuit. Cross-state switches between beam splitters were used to compensate for phase fluctuations between paths caused by fabrication errors. The detailed phase trimming method will be explained in Section III. Bar-state switches were used to guide photons in the desired direction.

III. Phase Trimming Method

This section details the method used for phase trimming. Fabrication errors in the widths of the Si waveguides cause phase differences in the paths between beam splitters. To realize an ideal QW circuit, the phase errors should be trimmed using the method shown here.

The phase trimming method starts with the green part in Fig. 4(a), which includes an interference loop with four adjustable phases ϕ_1, ϕ_2, ϕ_3 and ϕ_4, which can be individually

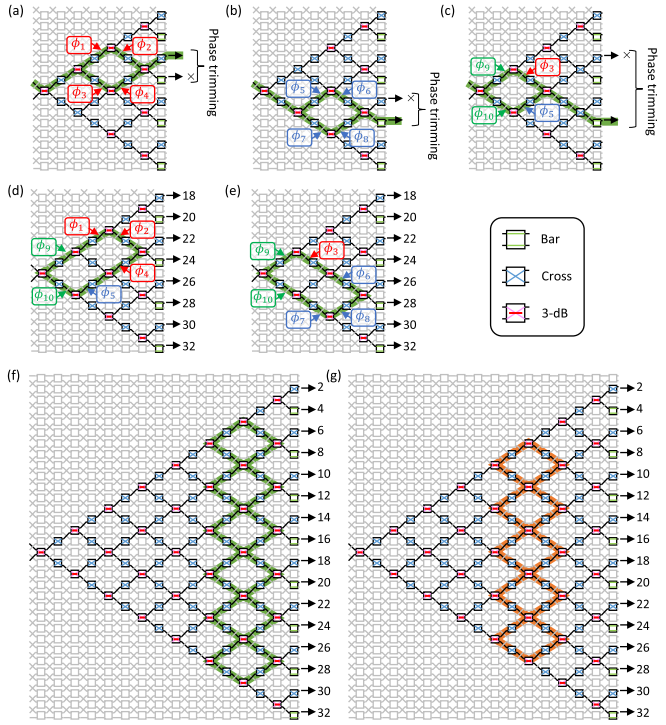

Fig. 4. (a)–(c) Phase trimming steps for 4-step QW circuit. (d)–(e) Schematic illustration of phase trimming of larger interference loops. (f) First and (g) second target interference loops for 8-step QW.

set by tuning the four cross-state switches on the interference loop so that both the upper and lower phase shifters [as shown in Fig. 1(a)] of a switch have the same amount of phase shift. This interference loop is the smallest that can be built in our switch circuit. A continuous-wave (CW) light of 1550 nm is used to observe constructive interference, which yields

$$\phi_1 + \phi_2 = \phi_3 + \phi_4 \quad (mod\ 2\pi). \tag{1}$$

In a similar manner, from Fig. 4(b) we obtain

$$\phi_5 + \phi_6 = \phi_7 + \phi_8 \quad (mod\ 2\pi). \tag{2}$$

Next, we consider the interference loop in Fig. 4(c). We adjust ϕ_9 and ϕ_{10} without changing ϕ_3 and ϕ_5 to satisfy the following constructive interference condition,

$$\phi_3 + \phi_9 = \phi_5 + \phi_{10} \quad (mod\ 2\pi). \tag{3}$$

Therefore,

$$\phi_1 + \phi_2 + \phi_9 = \phi_4 + \phi_5 + \phi_{10} \quad (mod\ 2\pi) \tag{4}$$

and

$$\phi_3 + \phi_6 + \phi_9 = \phi_7 + \phi_8 + \phi_{10} \quad (mod\ 2\pi) \tag{5}$$

ensure constructive interference of the interference loops in Figs. 4(d) and 4(e), respectively. The method is thereby completed. This is a simple trimming method in which each interferometer loop can be adjusted independently and separately. We can extend this method to any N-step QW circuit. For example, building an 8-step QW circuit starts with interference loops on the far right of the device (see the six interference loops marked

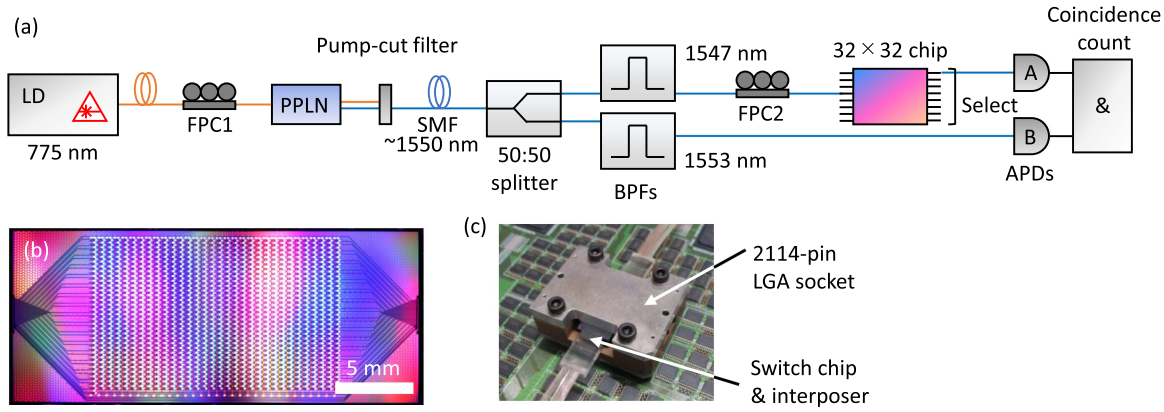

Fig. 5. (a) Illustration of experimental setup. A tunable 775-nm CW laser was used as a pump source to generate 1550-nm heralded single photons using SPDC. The single photons were filtered by 10 nm and input into the QW circuit. (b) Micrographic image of 32 × 32 switch. (c) Photograph of the packaged switch chip with a control circuit board.

in green in Fig. 4(f)). We monitor their interference signals one by one. Then, we move one step to the left and check the next five interference loops (marked in orange in Fig. 4(g)). Since the total number of interference loops to be tested is given by $(N-1)(N-2)/2$, building an N-step QW circuit requires $O(N^2)$ interference measurements.

IV. Results

Using the above method, we prepared QW circuits increasing in size up to 8-step QW circuits using CW light centered at 1550 nm with 16-channel power monitors. In this section, we show the results of the QW experiments using single photons.

A. Single-Photon Quantum Walk

Fig. 5(a) shows the setup used for the single-photon QW experiment. We input a 775 nm CW laser beam via a fiber-optic polarization controller (FPC1) to a periodically poled lithium niobate (PPLN) waveguide to generate 1550 nm photon pairs through an SPDC process. The two photons are split using a 50:50 splitter and filtered using band-pass filters (BPFs) having center wavelengths of 1547 nm and 1553 nm, respectively, with a 3-dB bandwidth of 10 nm. If the device bandwidth is narrow ($\ll$10 nm), the BPF widths should also be set to be narrow, significantly increasing the integration time. Achieving a broad device bandwidth is thus very important for shortening the integration time for the experiments.

After the BPF, the single photons are input to the 32 × 32 device. An optical micrograph of the device is shown in Fig. 5(b). The chip used was a flip-chip bonded to a ceramic interposer and inserted into an LGA socket, as shown in [11]. The heaters on the chip are controlled using pulse width modulation electrical signals from a control circuit board, as shown in Fig. 5(c). Because the chip was designed only for a transverse-electric (TE) mode, we used a fiber polarization controller (FPC2 in Fig. 5(a)) to adjust the input polarization.

The photons output from each output port (2′ to 32′) of the switch are guided to avalanche photodiode (APD) A. The idler photons are guided to APD B, and the difference between the click timings of the two APD channels is measured using a start-stop timer. The APDs are gated by a 4-MHz repetition frequency with a gate width of 2.5 ns. Our PILOSS switch has a fiber-to-fiber loss of approximately 10 dB. We set the integration time at 600 sec to suppress fluctuations in photon counting and secure enough counts at each output port. For example, a single-photon count of 1,545 was obtained when input 1 and output 32′ were connected as a single-pass transmission line.

We measured the output photon distribution from 1- to 8-step QWs using single photons. The results for the 4- and 8-step QWs are plotted in Figs. 6(a) and 6(b), respectively, in which the blue bars show the measured single photon distributions and the orange bars show the theoretical (ideal-case) photon distributions. These figures show that clear non-Gaussian photon distributions were observed as expected theoretically. The measured fidelity of the 3- to 8-step QWs using single photons are plotted as open red points in Fig. 6(c), where the fidelity is defined as follows [5],

$$F = \sum_i \sqrt{p_i q_i}, \tag{6}$$

where p_i and q_i correspond to the measured and theoretical photon distributions for output port i, respectively. The results for the 1- and 2-step QWs are not shown because these configurations do not include interference parts. The measured fidelity was $>$0.97 for the 8-step QW, showing the formation of precise interference. For reference, we inject coherent light from a tunable CW laser (200-kHz linewidth) and measure the fidelity for each QW setup by varying the center wavelengths, shown by the blue, orange and green points in Fig. 6(c). These results show a degradation of fidelity due to dispersion of the MZIs, i.e., single photons have lower fidelity values due to their broad bandwidth ($\sim$10 nm) compared to the CW laser (200 kHz), and are more sensitive to the dispersion of the device. The effect of bandwidth on the MZIs will be discussed in Section V.

B. Temporal Stability Measurement

Another important requirement of Si photonic circuits for large-scale quantum photonic experiments is temporal stability. To investigate this experimentally, we configured the device for an 8-step QW and continued taking measurements for 45 hours

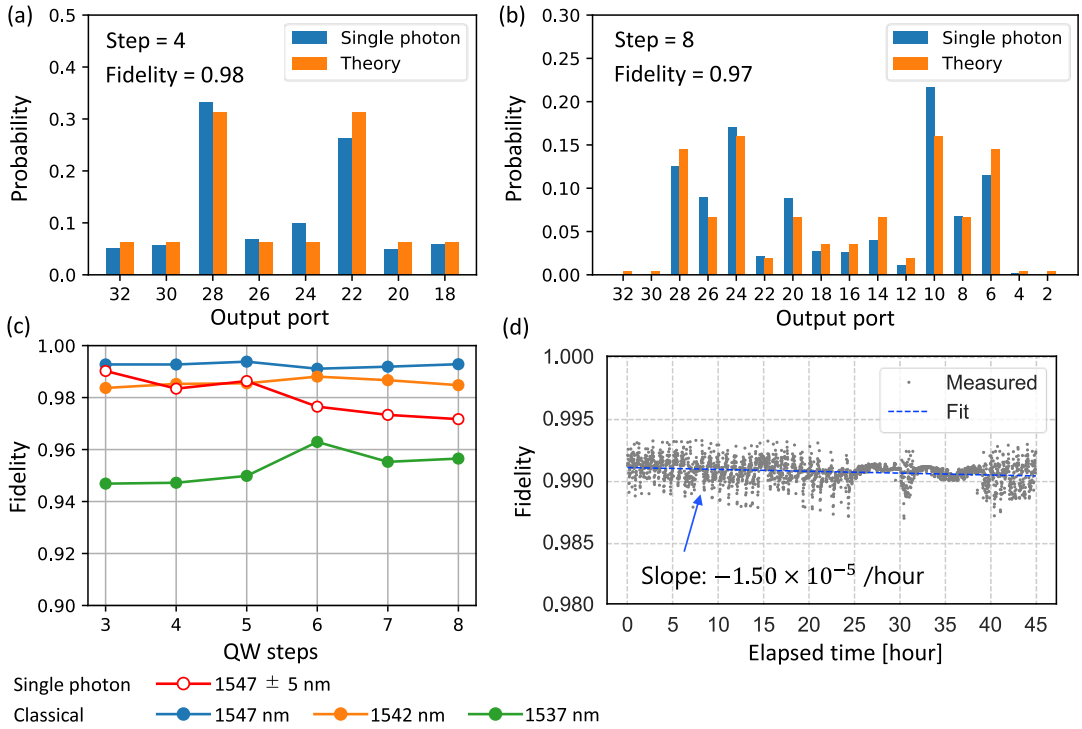

Fig. 6. Measured (blue) and theoretically calculated (orange) photon distributions for (a) 4-step QW and (b) 8-step QW. (c) Calculated fidelity for photon distributions measured with single photons (red) and coherent light (blue, orange, green). (d) Measured fidelity for 8-step QW as function of time up to 45 hours with coherent light input.

and calculated the fidelity. For this experiment, we used coherent CW light. The results are plotted as the gray points Fig. 6(d) and a linear fit to the points is plotted as the blue dashed line. The degradation rate for the fidelity was very low at -1.50×10^{-5} per hour, indicating that the 8-step QW circuit is stable for tens or hundreds of hours. In this particular case, we directly observed the long stability for more than 45 hours with this free-run test. We note that the time required to collect all the data including 2- to 8-step quantum walks was 21 hours. The breakdown of this time is given as follows. For each step, we monitored 16 output ports one by one for single-photon detection. The integration time was 600 sec/port × 16 port × 7 plus. Another 2 hours were required if we sum up all intervals used to change steps. Therefore, it totals 21 hours. We also note that the measurement could be greatly sped up, by a factor of 16, using 16 APDs to measure the relevant output ports simultaneously.

Room temperature changes are one of the sources of fidelity fluctuations observed in the graph. Because the device is designed for TE polarization alone, TM photons (or coherent light) are randomly scattered at the output ports. Although we adjust input photons to be TE-polarized, temperature change in fibers induces unwanted rotation of polarization, resulting in the observed fluctuations. This effect could be avoided by integrating on-chip polarizers. In the demonstrated experiments, no temperature stabilization systems were installed because of simple free-running operation. Therefore, we believe that fidelity fluctuations could also be mitigated by using temperature stabilization systems.

We note that desirable fidelity or phase error tolerance is very application specific. In general, the importance of fidelity measurement grows as we increase the number of photons (or 'walkers' for advanced QW experiments). For two photons, it can be connected to the quality of quantum entanglement [18].

V. Discussion

In this section, we discuss increasing the port count. With the current design of the 32 × 32 switch chip, the maximum possible number of steps is eight because the top and bottom MZIs have different waveguide lengths than the inner MZIs. However, this can be easily adjusted by the chip design up to a maximum possible number of QW steps of 16 with a 32 × 32 switch chip.

However, when increasing the number of steps, we need to consider the accumulation of splitting-ratio deviation of the MZIs due to the wavelength dependency, as shown in Fig. 2, which reduces the device bandwidth. We calculated the fidelity spectra for QW step numbers of 8, 16 and 32 in Fig. 7(a) considering the splitting-ratio deviation and wavelength dependency of the phase shifters. We used both FEM and CMT for the calculations. In Fig. 7(a), complex shapes of the spectra were observed due to interference between the paths, especially for $N = 16$ and $N = 32$. Specifically, asymmetric spectra arise from the wavelength dependency of the phase at the phase shifters. The results in Fig. 7(a) show the expected fidelity when a single-frequency CW laser beam is input to the system. To calculate the expected fidelity when broad bandwidth

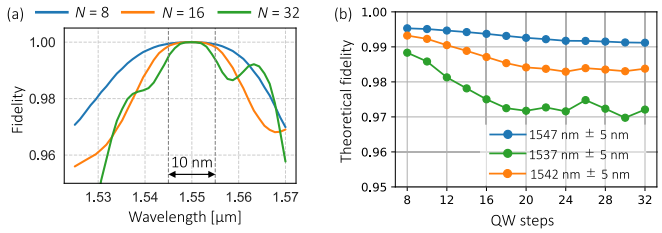

Fig. 7. Calculated fidelity spectra with QW steps of $N \geq 8$ for (a) single-frequency tunable lasers and (b) 10-nm SPDC single photons.

(approximately 10 nm) single photons are input to the system, we calculated the convolution of Fig. 7(a) and the 10-nm bandwidth filter spectrum used in the experiments. The results are shown in Fig. 7(b), and indicate the expected single-photon QW fidelity with steps varying from 8 to 32. The figure shows that the fidelity decreases with increasing number of steps due to accumulation of splitting ratio deviation and the wavelength dependency of the phase shifters, as experimentally observed (see open red points in Fig. 6(c)). However, the theoretical fidelity for the 32-step QW is still high and SPDC single photons with 10-nm bandwidth are feasible for the large-scale implementation of quantum circuits.

Increasing the bandwidth of the device would be very important to improve fidelity values for heralded single photons. This can be achieved by, for example, using adiabatic waveguide couplers to make the 50:50 couplers broadband for each MZI [19].

Regarding the insertion loss of the photonic circuit, we can expect a further reduction in fiber-to-chip coupling loss by using technologies such as ultra high-Δ PLC connectors [12]. The on-chip loss can also be reduced by using a small form-factor design [20].

We achieved highly accurate inter-chip reproducibility. The ArF immersion lithography yields small phase errors in each MZI, enabling small trimming power of $\sim$1.5 mW per MZI [12]. Moreover, we fabricate tens of chips at the same time from a single 300-mm wafer. Therefore, not only 'as-fabricated' characteristics are similar, but also unwanted errors are similar. The latter could be easily trimmed because of their uniformity across the wafer. We consider that these points positively work for reproducibility.

VI. Conclusion

In this paper, we demonstrated the broad bandwidth and time-stable characteristics of a large-scale Si photonics circuit, namely a 32 $\times$ 32 PILOSS switch. We observed very high ($>$0.97) fidelity even with single photons with a bandwidth of approximately 10 nm. We also measured the long-term stability of an 8-step QW for more than 45 hours using coherent light. These results are encouraging for the use of large-scale Si photonic circuits in complex quantum photonics experiments including not only QWs, but also Boson sampling and quantum phenomena.

References

[1] F. Flamini, N. Spagnolo, and F. Sciarrino, "Photonic quantum information processing: A review," *Rep. Prog. Phys.*, vol. 82, no. 1, 2018, Art. no. 016001.

[2] X. Qiang et al., "Large-scale silicon quantum photonics implementing arbitrary two-qubit processing," *Nature Photon.*, vol. 12, no. 9, pp. 534–539, 2018. [Online]. Available: http://dx.doi.org/10.1038/s41566-018-0236-y

[3] J. Carolan et al., "Universal linear optics," *Science*, vol. 349, no. 6249, pp. 711–716, 2015. [Online]. Available: http://www.sciencemag.org/cgi/doi/10.1126/science.aab3642

[4] H.-S. Zhong et al., "Phase-programmable gaussian boson sampling using stimulated squeezed light," *Phys. Rev. Lett.*, vol. 127, Oct. 2021, Art. no. 180502. [Online]. Available: https://link.aps.org/doi/10.1103/PhysRevLett.127.180502

[5] N. C. Harris et al., "Quantum transport simulations in a programmable nanophotonic processor," *Nature Photon.*, vol. 11, no. 7, pp. 447–452, 2017. [Online]. Available: http://dx.doi.org/10.1038/nphoton.2017.95

[6] B. Do et al., "Experimental realization of a quantum quincunx by use of linear optical elements," *J. Opt. Soc. Amer. B*, vol. 22, no. 2, pp. 499–504, 2005.

[7] H. B. Perets, Y. Lahini, F. Pozzi, M. Sorel, R. Morandotti, and Y. Silberberg, "Realization of quantum walks with negligible decoherence in waveguide lattices," *Phys. Rev. Lett.*, vol. 100, no. 17, 2008, Art. no. 170506.

[8] A. Schreiber, K. N. Cassemiro, V. Potoček, A. Gábris, I. Jex, and C. Silberhorn, "Decoherence and disorder in quantum walks: From ballistic spread to localization," *Phys. Rev. Lett.*, vol. 106, May 2011, Art. no. 180403. [Online]. Available: https://link.aps.org/doi/10.1103/PhysRevLett.106.180403

[9] A. Crespi et al., "Anderson localization of entangled photons in an integrated quantum walk," *Nature Photon.*, vol. 7, no. 4, pp. 322–328, 2013.

[10] S. E. Venegas-andraca, "Quantum walks: A comprehensive review," *Quantum Inf. Process.*, no. 11, pp. 1015–1106, 2012.

[11] K. Tanizawa et al., "Ultra-compact 32 $\times$ 32 strictly-non-blocking Si-wire optical switch with fan-out LGA interposer," *Opt. Exp.*, vol. 23, no. 13, pp. 17599–17606, 2015. [Online]. Available: https://www.osapublishing.org/abstract.cfm?URI=oe-23-13-17599

[12] K. Suzuki et al., "Low insertion loss and power efficient 32 $\times$ 32 silicon photonics switch with Extremely-High-Δ PLC connector," in *Proc. Opt. Fiber Commun. Conf. Exp.*, 2018, pp. 1–3. [Online]. Available: https://www.osapublishing.org/abstract.cfm?URI=OFC-2018-Th4B.5

[13] K. Tanizawa et al., "Silicon photonic 32 $\times$ 32 strictly-non-blocking blade switch and its full path characterization," in *Proc. 21st OptoElectron. Commun. Conf.*, 2016, pp. 1–3.

[14] W. R. Clements, P. C. Humphreys, B. J. Metcalf, W. S. Kolthammer, and I. A. Walsmley, "Optimal design for universal multiport interferometers," *Optica*, vol. 3, pp. 1460–1465, 2016.

[15] R. Konoike, A. Yoshizawa, S. Namiki, and K. Ikeda, "Demonstration of 8-step single-photon quantum walk using 32$\times$32 reconfigurable silicon photonics switch," in *Proc. Conf. Lasers Electro- Opt.*, 2020, pp. 1–2.

[16] Y. Ma et al., "Ultralow loss single layer submicron silicon waveguide crossing for SOI optical interconnect," *Opt. Exp.*, vol. 21, no. 24, pp. 29374–29382, 2013.

[17] R. Konoike et al., "Gain-integrated 8$\times$8 silicon photonics multicast switch with on-chip 2 $\times$ 4-ch. SOAs," *J. Lightw. Technol.*, vol. 38, no. 11, pp. 2930–2937, 2020.

[18] H.-J. Briegel, W. Dür, J. I. Cirac, and P. Zoller, "Quantum repeaters: The role of imperfect local operations in quantum communication," *Phys. Rev. Lett.*, vol. 81, pp. 5932–5935, Dec. 1998. [Online]. Available: https://link.aps.org/doi/10.1103/PhysRevLett.81.5932

[19] M. A. Tran, C. Zhang, and J. E. Bowers, "A broadband optical switch based on adiabatic couplers," in *Proc. IEEE Photon. Conf.*, 2016, pp. 755–756.

[20] R. Konoike, K. Suzuki, S. Namiki, H. Kawashima, and K. Ikeda, "Ultra-compact silicon photonics switch with high-density thermo-optic heaters," *Opt. Exp.*, vol. 27, no. 7, pp. 10332–10342, 2019.

Ryotaro Konoike received the M.Eng. and Ph.D. degrees from the Department of Electronic Science and Engineering, Kyoto University, Kyoto, Japan, in 2014 and 2017, respectively. He studied the integration of manipulation of photons on a photonic crystal chip containing multiple coupled nanocavities with Kyoto University.

He is currently a Researcher with the National Institute of Advanced Industrial Science and Technology, Tokyo, Japan. His research interests include optical switches and integrated silicon optical circuits.

Dr. Konoike was the recipient APL Photonics Future Luminary Award in 2020.

Akio Yoshizawa received the M.E. and Ph.D. degrees from the University of Tsukuba, Tsukuba, Japan, in 1990 and 1996, respectively.

He joined the Electrotechnical Laboratory (ETL) in 1990. The ETL and other research institutes were reorganized in 2001 to become the National Institute of Advanced Industrial Science and Technology (AIST). His affiliation has changed to the AIST. He is currently a Senior Research Scientist studying quantum technologies such as quantum key distribution, single-photon detection, entanglement generation and manipulation, quantum diamond sensing and quantum-inspired metaheuristic algorithms for optimization problems. From 2007 to 2012, he was also a part-time lecturer with the University of Tsukuba. His research interests include optical frequency-domain reflectometry and frequency-shifted feedback lasers.

Dr. Yoshizawa is the Senior Member of *Optica* and Member of the *JSAP*.

Shu Namiki (Fellow, IEEE) received the M.S. and Dr.Sci. degrees in applied physics from Waseda University, Tokyo, Japan, in 1988 and 1998, respectively.

From 1988 to 2005, he was with Furukawa Electric Co., Ltd., Tokyo, Japan, where he developed award-winning high-power pump lasers and patented multiwavelength pumped-fiber Raman amplifiers. From 1994 to 1997, he was a Visiting Scientist with the Massachusetts Institute of Technology, Cambridge, MA, USA, where he studied mode-locked fiber lasers and ultra-short pulses in fibers. In 2005, he moved to the National Institute of Advanced Industrial Science and Technology, Tsukuba, Japan, where he was the Chair of Executive Committee of a ten-year National Project called Vertically Integrated Center for Technologies of Optical Routing toward Ideal Energy Savings in collaboration with ten telecom-related companies, and is currently the Director of Platform Photonics Research Center. He has authored or coauthored more than 500 conference presentations, papers, book chapters, articles, and patents. His research interests include software defined dynamic optical path networking and their enabling devices such as nonlinear fiber-optics and silicon photonics. He was an Associate Editor and Advisory Editor for the journal *Optics Express* and the Co-Editor-in-Chief of *IEICE Transactions on Communications*. He was with the Technical Committee for OFC, ECOC, CLEO, OECC, and OAA and was the Program Co-Chair of OFC 2015 and General Co-Chair of OFC 2017.

Dr. Namiki is a Fellow of Optica and IEEE. He is a member of the Institute of Electronics, Information, and Communication Engineers, and the Japan Society of Applied Physics.

Kazuhiro Ikeda (Member, IEEE) received the B.E. and M.E. degrees in precision science from the Osaka University, Suita, Japan, in 1998 and 2000, respectively, and the Ph.D. degee in electrical engineering (Photonics) from the University of California, San Diego, La Jolla, CA, USA, in 2008. His doctoral thesis was on nonlinear optical responses in silicon nitride and amorphous silicon and sidewall corrugated waveguide devices, all for silicon photonics applications.

From 2000 to 2004, he worked for the Furukawa Electric Co., Ltd., Tokyo, Japan, on polarization controllers and polarization mode dispersion compensators for optical fiber communications. In 2009, he joined the Graduate School of Materials Science, Nara Institute of Science and Technology (NAIST), Ikoma, Japan, as an Assistant Professor, where he studied opto-spintronics and plasmonic microresonators for semiconductor lasers. Since 2014, he has been a Research Group Leader with the National Institute of Advanced Industrial Science and Technology, Tsukuba, Japan. His research interests include silicon photonic integrated circuits and hybrid nanophotonics on silicon.

Dr. Ikeda is also the Senior Member of *Optica*, Member of the IEICE, JSAP, IEEE Photonics Society. He was the recipient of World Cultural Council (WCC) Special Recognition 2019.